CEO Clinical and Experimental Otorhinolaryngology Vol. 16, No. 2: 184-197, May 2023
https://doi.org/10.21053/ceo.2022.01760
pISSN 1976-8710 eISSN 2005-0720

Original Article

Mitochondrial Ribosomal Protein L14 Promotes Cell Growth and Invasion by Modulating Reactive Oxygen Species in Thyroid Cancer

Hae Jong Kim[1,*] · Quoc Khanh Nguyen[1,*] · Seung-Nam Jung[2] · Mi Ae Lim[2] · Chan Oh[1]
Yudan Piao[1] · YanLi Jin[1] · Ju-Hui Kim[2] · Young Il Kim[3] · Yea Eun Kang[4]
Jae Won Chang[1,2] · Ho-Ryun Won[1,2] · Bon Seok Koo[1,2]

[1]*Department of Medical Science, Chungnam National University College of Medicine, Daejeon, Korea*
[2]*Department of Otolaryngology-Head and Neck Surgery, Chungnam National University College of Medicine, Daejeon, Korea*
[3]*Department of Radiation Oncology, Chungnam National University Sejong Hospital, Sejong, Korea*
[4]*Division of Endocrinology and Metabolism, Department of Internal Medicine, Chungnam National University College of Medicine, Daejeon, Korea*

Objectives. The mitochondrial ribosomal protein L14 (MRPL14) is encoded by a nuclear gene and participates in mitochondrial protein translation. In this study, we aimed to investigate the role of MRPL14 in thyroid cancer.

Methods. We investigated the association between MRPL14 expression and clinicopathological features using The Cancer Genome Atlas (TCGA) and Chungnam National University Hospital (CNUH) databases. Functional studies of MRPL14, including proliferation, migration, invasion, mitochondrial oxidative phosphorylation and reactive oxygen species (ROS) production, were performed in papillary thyroid cancer (PTC) cell lines (B-CPAP and KTC-1).

Results. Based on the TCGA dataset, PTC tissues lost mitochondrial integrity and showed dysregulated expression of overall mitoribosomal proteins (MRPs) compared with normal thyroid tissues. Of 78 MRPs, MRPL14 was highly expressed in thyroid cancer tissues. MRPL14 overexpression was significantly associated with advanced tumor stage, extrathyroidal extension, and lymph node metastasis. MRPL14 increased cell proliferation of thyroid cancer and promoted cell migration via epithelial-mesenchymal transition-related proteins. Moreover, MRPL14 knockdown reduced the expression of oxidative phosphorylation complex IV (MTCO1) and increased the accumulation of ROS. Cotreatment with a ROS scavenger restored cell proliferation and migration, which had been reduced by MRPL14 knockdown, implying that ROS functions as a key regulator of the oncogenic effects of MRPL14 in thyroid cancer cells.

Conclusion. Our findings indicate that MRPL14 may promote cell growth, migration, and invasion by modulating ROS in thyroid cancer cells.

Keywords. *Papillary Thyroid Cancer; Mitoribosomal Protein 14; Reactive Oxygen Species; Cancer Progression*

INTRODUCTION

Thyroid cancer is the most common type of endocrine-related cancer, and its incidence has been increasing over the last few decades [1,2]. Thyroid cancer can be classified into several categories in accordance with its histopathological features: papillary, follicular, medullary, poorly differentiated, and anaplastic. Papillary thyroid cancer (PTC) is the most frequently occurring thyroid cancer, accounting for 80% of all malignant thyroid tumors [3,4]. Most patients with PTC have a good prognosis and a

• Received December 21, 2022
Revised February 17, 2023
Accepted February 23, 2023

• Corresponding author: **Bon Seok Koo**
Department of Otolaryngology-Head and Neck Surgery, Chungnam National University College of Medicine, 266 Munhwa-ro, Jung-gu, Daejeon 35015, Korea
Tel: +82-42-280-7695, Fax: +82-42-253-4059
Email: bskoo515@cnuh.co.kr

*These authors contributed equally to this work.

low mortality rate. However, PTC commonly metastasizes to the lymph nodes and has high locoregional recurrence rates [5]. Moreover, anaplastic thyroid cancer (ATC), an undifferentiated type of thyroid cancer, displays the most aggressive clinical behavior because of its wide-ranging local invasion of surrounding tissue, metastasis to distant organs, and speedy growth. Consequently, it has the worst prognosis among thyroid cancers, with a median overall survival of only 2.5–6 months [6]. Therefore, it is necessary to identify novel molecular biomarkers and potential therapeutic targets related to the aggressiveness of thyroid cancer, which may be helpful for improving treatment [7].

Mitochondria are dynamic organelles that manufacture the energy demanded by cells and play an important role in cellular energy metabolism. Several studies have reported that mitochondrial disorders or dysfunction might be related to the origin of numerous diseases, including cancer [8]. Thirteen mitochondrial proteins, all of which are essential for oxidative phosphorylation (OXPHOS), are synthesized in the specialized translation machinery known as the mitochondrial ribosome (mitoribosome). The human mitoribosome consists of two mitoribosomal RNA components encoded by mitochondrial DNA and 82 mitoribosomal proteins (MRPs) encoded by nuclear DNA [9,10]. Consequently, the balanced expression of ribosomal RNA and MRPs and their appropriate formation are essential for the control of OXPHOS activity and the consequent energy production. Many studies have reported that altered expression of several MRPs was closely related to the development, progress, and metastasis of many cancer types [11]. For instance, MRPL11 expression was found to be reduced in the primary tumor tissues of head and neck squamous cell cancer (HNSCC), prompting MRPL11 to be regarded as a latent biomarker for HNSCC [12]. A study reported increased MRPS16 expression in the primary tumor tissues of glioma and considered it as a prospective novel target for the medical cure of glioma [13]. In addition, MRPS23 and MRPS6 exert pro-carcinogenic functions in breast cancer [14]. However, the mechanisms underlying the contribution of changes in MRPs to cancer progression are still poorly understood.

HIGHLIGHTS

- In The Cancer Genome Atlas-papillary thyroid cancer database, MRPL14 overexpression was significantly associated with advanced tumor stage, extrathyroidal extension, and lymph node metastasis.
- Mitochondrial ribosomal protein L14 (MRPL14) increased cell proliferation of thyroid cancer and promoted cell migration via epithelial-mesenchymal transition-related proteins.
- MRPL14 knockdown reduced the expression of oxidative phosphorylation complex IV (MTCO1) and increased the accumulation of reactive oxygen species (ROS).
- Our findings indicate that MRPL14 may promote cancer progression and metastasis through modulating ROS in thyroid cancer.

Mitochondrial ribosomal protein L14 (MRPL14) is a 16-kDa protein encoded by the MRPL14 gene located at 6p21.1. MRPL14 plays an important role in promoting the biogenesis of the mitochondrial large ribosomal subunit and mitochondrial translation [15]. However, the role of MRPL14 in thyroid cancer has not yet been clarified. In a study of The Cancer Genome Atlas (TCGA) data, we recently discovered that MRPL14 was highly expressed in PTC tissues and showed the potential to be an oncogene. Therefore, in this study, we investigated the molecular mechanism of MRPL14 associated with thyroid cancer progression and metastasis by conducting transgene experiments with cultured thyroid cancer cells.

MATERIALS AND METHODS

Cell lines and reagents

The human thyroid cancer cell lines B-CPAP, TPC-1, KTC-1, FRO, SW1736, and 8505C, and the normal thyroid cell line Nthy-ori3.1 were helpfully contributed by Professor Yea Eun Kang (Chungnam University). The B-CPAP, TPC-1, FRO, SW1736, 8505C, and Nthy-ori3.1 cell lines were cultured in RPMI-1640 medium (Gibco, #LM 011-03). The KTC-1 cell line was cultured in high-glucose Dulbecco's Modified Eagle medium (DMEM; Gibco, #LM 001-05). All cell lines were supplied with 10% fetal bovine serum (FBS; Gibco, #16000044), and 1% penicillin-streptomycin (Gibco, #15140122) on 10-cm tissue culture plates. In all experiments, cells were maintained at 37 °C in a humidified 5% CO_2, 95% air atmosphere.

Data and preprocessing

The reads were aligned to the UCSC Homo sapiens reference genome (GRCh37/hg19) using TopHat2 v2.1.5 (https://ccb.jhu.edu/software/tophat/index.shtml). The default TopHat parameter options were used. To analyze the differentially expressed gene (DEG) profiles between the compared groups (normal vs. tumor), the Tuxedo protocol was used [16]. The aligned reads were processed through Cufflinks v2.2.1 (https://github.com/cole-trapnell-lab/cufflinks), which is based on the fragments per kilobase of transcript per million mapped fragments (FPKM), and unbiased, normalized RNA-sequencing fragment counts were used to analyze the relative transcript levels [16]. Gene transfer format (GTF) files were generated to quantitatively compare the transcript levels in each sample to those in a reference GTF file. Next, we used Cuffdiff to calculate the differences in the FPKMs between each group. False discovery rate-adjusted P-values <0.05 were calculated through the Benjamini-Hochberg multiple testing method [17]. We also investigated the crucial role of MRPL14 using the TCGA and Chungnam National University Hospital (CNUH) databases. In addition, we confirmed DEGs by establishing two groups based on the MRPL14 expression level in tu-

mors in the TCGA and CNUH databases. DEGs with Benjamini-Hochberg-corrected values <0.05 were considered statistically significant. Heat maps were constructed with PermutMatrix ver. 1.9.3 (http://www.lirmm.fr/~caraux/PermutMatrix/).

Profiling of the MRP transcriptome

We performed a transcriptome profiling of 78 MRPs. First, to select variable MRPs among these 78 MRPs, we applied a cut-off of a maximum absolute deviation >0.25 for further analysis. To identify the MRP defect-associated signature in thyroid cancer, we carried out the permutation *t*-test between tumor and normal samples and assigned selected MRPs into three categories: up-MRPs, dn-MRPs, and other-MRPs, according to the false discovery rate (FDR) and fold change (FC) (FDR <0.05 & FC >0.25, FC <–0.25, or –0.25< FC <0.25, respectively).

Patients' samples and ethics statement

To analyze the transcriptome and identify DEGs, RNA was extracted from tumor tissue samples and paired non-tumor tissue samples from thyroid cancer patients (n=364) in the CNUH database. Extracted RNA (1 μg) was used to construct RNA libraries using the TruSeq stranded mRNA sample preparation kit v2 (Illumina) according to the manufacturer's protocols. The library quality was analyzed with an Agilent 2100 Bioanalyzer using the Agilent DNA 1000 kit. Samples from five patients diagnosed with PTC at CNUH were included in the study. Paired tumor and normal thyroid tissues were obtained from patients with PTC. All samples were gathered from patients after they provided informed consent according to The Institutional Guidelines of Chungnam National University Hospital.

The protocol for this study was approved by the Institutional Review Board of CNUH (No. 2017-07-005). Human tissues were homogenized in radioimmunoprecipitation assay (RIPA) buffer and processed following the immunoblotting analysis protocol.

RNA isolation and real-time polymerase chain reaction

Total cellular RNA was extracted using TRIzol (Invitrogen) and cDNA was synthesized with 2 μg of total RNA and TOPscript RT DryMIX (Enzynomics Inc.) according to the manufacturer's instructions. Amplification was carried out using SYBR Green quantitative polymerase chain reaction (qPCR) master mix (Thermo Fisher Scientific). The PCR reactions were performed for 40 cycles at 95 °C for 15 seconds, 60 °C for 1 minute and 72 °C for 1 minute. The primer sequences were as follows: MRPL14-F: 5´-GAA GAA AAA GGC GCT CAT TG-3´/MRPL14-R: GAG GAC CAC GTT GTT GGA GT-3´; GAPDH-F: 5´-ACC CAG AAG ACT GTG GAT GG-3´/GAPDH-R: 5´-TTC TAG ACG GCA GGT CAG GT-3´. The cycle threshold (Ct) values provided from real-time PCR instrumentation were imported into Microsoft Excel. We used the $2^{-\Delta\Delta Ct}$ model for relative quantification of real-time qPCR fold changes.

Small interfering RNA transfection

Cells were seeded at a density of 1×10^5/well in six-well plates and then cultured for 24 hours to achieve 65%–70% confluence. The following day, transient transfection was conducted using Lipofectamine RNAi MAX reagent (Invitrogen, #56532) following the manufacturer's standardized protocol. Mitochondrial ribosomal protein L 14 small interfering RNA (siRNA) (AM-16708) was a pool of two dissimilar siRNA duplexes: AM16708A:(sense: 5´-CGA AUU AAG ACA CCC AUC Ctt-3´; antisense: 5´-GGA UGG GUG UCU UAA UUC Gtg-3´), AM16708B: (sense: 5´-GGU GGG CGA CCA GAU ACU Att-3´; antisense: 5´-UAG UAU CUG GUC GCC CAC Ctt-3´) or negative control siRNA (#SN-1003), purchased from Bioneer. The medium was changed after 7–8 hours, and transfected cells were incubated at 37 °C for an added 48 hours. An immunoblot assay was conducted to assess the efficacy and efficiency of siRNA knockdown.

Cell proliferation assay

B-CPAP and KTC-1 cells were seeded onto 96-well plates at a denseness of 8,000 cells per well in 100 μL. The following day, the cells were treated with a 50 nM concentration of MRPL14 siRNA (Invitrogen) for 48 hours. Cell viability was measured using the Cell Counting Kit-8 cell proliferation reagent (DOJINDO Lab., #CK04) as formerly reported. The optical density of each culture well was measured at 450 nm using an enzyme-linked immunosorbent assay reader. The experiments were repeated three times. The unpaired Student *t*-test was used for statistical analysis.

Western blot analysis

Cells were plated at 15×10^4 cells/cm^2; the next day, they were treated with reagent and incubated for 48 hours at 37 °C, cleaned with cold Dulbecco's phosphate-buffered saline (DPBS), and harvested. All cells were dissolved using the RIPA cell lysis buffer (Thermo Fisher Scientific, #89900) supplied with phosphatase inhibitors (Thermo Fisher Scientific, #78427) and a protease inhibitor cocktail (Roche, #11836170001). Total protein concentration was determined using a BCA Protein Assay Kit (Thermo Fisher Scientific, #23228). For western blots, the proteins were denatured by boiling. Proteins were separated using sodium dodecyl sulfate-polyacrylamide gel electrophoresis (SDS-PAGE) gel electrophoresis and electrotransferred onto polyvinylidene fluoride membranes (Merck Millipore). The membrane was blocked in Tris-buffered saline, 0.1% Tween 20 (TBST) containing 5% skim milk powder for 1 hour at room temperature. After being cleaned with TBST, the membranes were incubated with primary anti-human antibodies overnight at 4 °C. The following day, after three cleans with TBST, the membrane was then incubated with the matching horseradish peroxidase-linked secondary antibodies (1:1,000; Cell Signaling Technology Inc.) for 2 hours at room temperature. The blots were cleaned and developed using enhanced chemiluminescence (Bio-Rad). The experi-

ments were repeated three times. The unpaired Student *t*-test was used for statistical analysis.

Cell migration and invasion (transwell) assay

Cell migration and invasion were determined using transwell assays. Simply, transwell membranes (24-well, SPL) were covered with Matrigel for 6 hours for the invasion assay, or without Matrigel for the migration assay. B-CPAP and KTC-1 cells were transfected for 48 hours before the transwell assay. After 48 hours, cells transfected with negative control siRNA or IC gene siRNA (5×10^4 in 150 μL serum-free medium) were added to the upper chamber. Next, 450 μL medium containing 10% FBS was added to the lower chamber. The chamber was incubated for 24 hours at 37 °C in 5% CO_2. Lastly, the cells adhering to the upper surface of the membrane were removed with a cotton swab. The invading or migrating cells, which adhered to the lower surface, were dyed with 1% crystal violet solution and counted in four representative fields by optical microscopy (×100 magnification). The experiments were repeated three times. The unpaired Student *t*-test was used for statistical analysis.

Reactive oxygen species assay

The level of intracellular reactive oxygen species (ROS) was measured by flow cytometry using 2,7-dichlorofluorescein diacetate (H2DCFH-DA, Invitrogen). The cells seeded in a 6-well plate, were cleaned twice with phosphate-buffered saline (PBS) post-treatment and co-incubated with serum-free culture medium containing 10 μM H2DCFH-DA (20 minutes, 37 °C, in dark conditions). The cells were cleaned thrice with DPBS and the cells were detached using trypsin-EDTA (ethylenediaminetetraacetic acid) solution. All the samples were centrifuged and the supernatants were resuspended in 500 μL of PBS. The fluorescence intensity was measured using a flow cytometer (535 nm emission, 485 nm excitation). The experiments were repeated three times. The unpaired Student *t*-test was used for statistical analysis.

Gene set enrichment analysis for pathway analysis

MRPL14 and its co-expressed genes were investigated by analyzing the CHNU database. Then, the c2.Cp.kegg.V7.5.symbol.gmt and c5.all.V7.5.1Symbols.gmt gene datasets were downloaded from the MsigDB and gene set enrichment analysis (GSEA) portal. The expression data were analyzed using the GSEA portal version 3.0. The enrichment analysis was conducted, and genes were displayed in descending order from high to low enrichment scores. The gene clusters with an FDR <0.25 and *P*-value <0.05 were considered to be significantly enriched genes.

Statistical analyses

Statistical analyses were conducted using SPSS ver. 22.0.0. (IBM Corp.) and GraphPad Prism 6 (GraphPad). The unpaired Student *t*-test was used for statistical analysis. Data from three independent experiments were expressed as the mean±standard deviation. A *P*-value <0.05 was considered to indicate statistical significance.

RESULTS

Abnormal expression of MRPs in PTC patients

To investigate the role of MRPs in thyroid cancer progression, we first performed a transcriptome analysis using the tumor and normal samples from PTC patients in the TCGA cohort (Fig. 1A). Intriguingly, we discovered that the distribution of the overall expression levels of 78 MRPs was not different between the tumor and normal samples (Fig. 1B). However, the tumor group displayed more variable expression levels of MRPs in each sample than observed in the normal group (Fig. 1C and D). These results indicate that the tumor group had lost its mitoribosomal integrity and displayed dysregulated expression of MRPs, while the normal group had moderate mitoribosomal integrity. The TCGA data could be divided into three individual MRP signatures (9 up-MRPs, 3 down-MRPs, and 20 other-MRPs) by comparing the MRP expression between tumor and normal samples (permuted Student *t*-test $P<0.05$ and fold change >0.25, Methods) (Fig. 1A). Subsequently, gene set variation analysis was conducted to measure the expression enrichment of these signatures in each of the tumor samples (Fig. 1E). Interestingly, most thyroid cancer samples showed higher expression of up-MRPs and lower expression of the down-MRPs. Thus, we suggest that the dysregulated MRP expression in tumors could play crucial roles in thyroid cancer development and progression.

MRPL14 expression is correlated with aggressive clinicopathological features

We identified DEGs for MRPs between the tumor and normal samples in the TCGA PTC cohort and drew a volcano plot (Fig. 2A). Among nine up-MRPs with potential as oncogenes, MRPL14 was the most upregulated gene, with dramatically higher expression in tumor samples than in normal samples (Fig. 2B). Next, to determine the significance of MRPL14 expression using integrative genome analysis, we verified the correlation between MRPL14 expression level and clinicopathological parameters using the TCGA thyroid cancer cohort. The patients were separated based on the top 25% and bottom 25% of gene expression. As indicated in Table 1, high MRPL14 expression levels (top 25%) were associated with patient age, T stage, extrathyroidal extension, lymph node metastasis, and American Joint Committee on Cancer stage. To further investigate the clinical significance of MRPL14 levels in thyroid cancer patients, we conducted a comparative transcriptome analysis of PTC samples (n=364) from the CNUH cohort. The expression of the MRPL14 gene in thyroid cancer tissues was significantly higher than in normal thyroid tissues (Fig. 2C). The MRPL14 protein was also overexpressed in thyroid cancer tissues relative to normal tissue from five PTC pa-

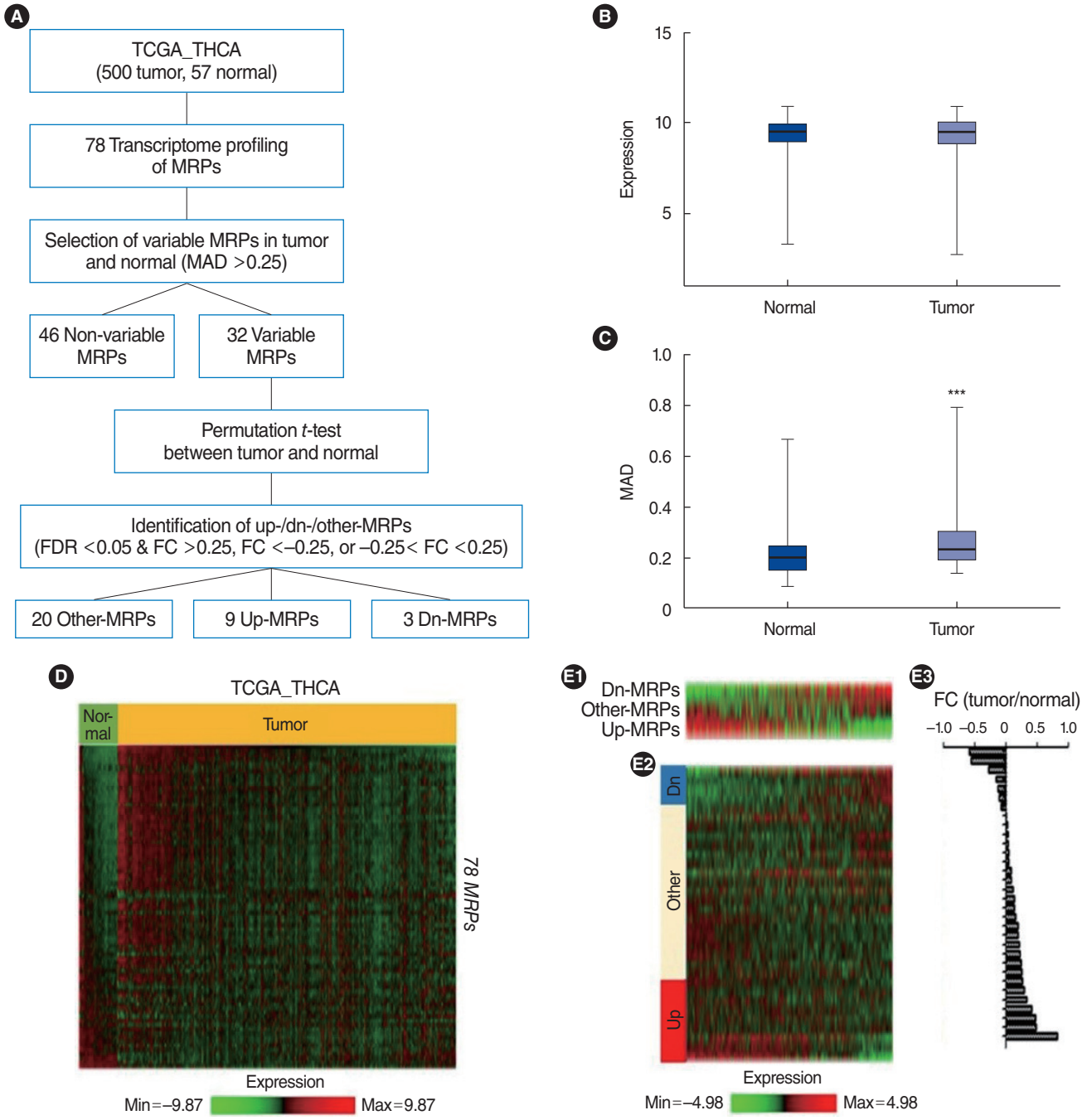

Fig. 1. Abnormal expression of mitoribosomal proteins (MRPs) in The Cancer Genome Atlas (TCGA) patients with thyroid cancer (THCA). (A) Schematic diagram of the analysis of MRPs to define three distinctive signatures (up-MRPs, dn-MRPs, and other-MRPs). (B) Comparison of MRP expression between tumor and normal samples. (C) Comparison of the maximum absolute deviation (MAD) among MRPs' expression between the thyroid cancer and normal group. (D) Heatmap displays the expression of 78 MRPs in 500 tumor samples and 57 normal samples from the TCGA thyroid cancer cohort. (E) Enrichment of three distinctive signatures (up-MRPs, dn-MRPs, and other-MRPs) in thyroid cancer patients (E1). Heatmap displays the expression of various MRPs (n=32) in thyroid cancer patients (E2). Bar graph shows the fold change in the expression of variable MRPs (n=32) between the tumor and normal samples (E3). FDR, false discovery rate; FC, fold change. ***P<0.001.

tients, which aligned with the MRPL14 mRNA expression results in the CNUH thyroid cancer cohort (Fig. 2D). These results suggest that high expression of MRPL14 is related to markers of tumor aggressiveness.

MRPL14 significantly promotes the progression of thyroid cancer cells

To examine the role of MRPL14, we first observed the expression levels of MRPL14 in thyroid cancer cell lines. Cell lysates

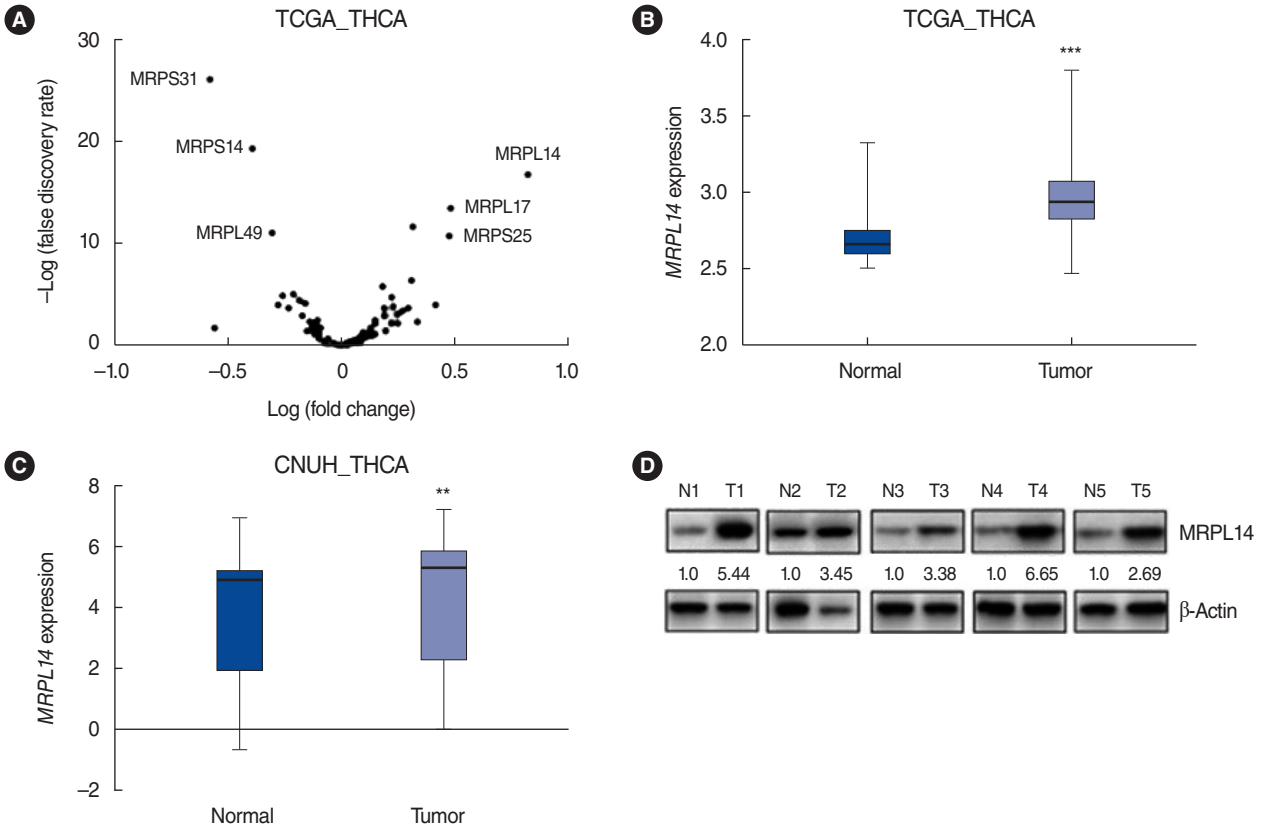

Fig. 2. *MRPL14* is highly overexpressed in The Cancer Genome Atlas (TCGA) and Chungnam National University Hospital (CNUH) thyroid cancer (THCA) cohort. (A) Volcano plot showing mitoribosomal protein (MRP) genes in the TCGA THCA cohort. (B) *MRPL14* expression levels in 500 tumor and 57 normal samples in the TCGA THCA dataset. (C) Graph showing MRP genes in 364 tumor samples and 244 normal samples from the CNUH_THCA cohort. (D) The protein levels of mitochondrial ribosomal protein L14 (MRPL14) in five tumor–normal pairs were detected by immunoblot analysis. Values are presented as mean±standard error of the mean. ***P*<0.01, ****P*<0.001.

were prepared from a normal cell line (Nthy-ori 3.1), PTC cell lines (B-CPAP, TPC-1, KTC-1), and ATC cell lines (FRO, SW1736, 8505C). We found that the mRNA levels of *MRPL14* were higher in most thyroid cancer cell lines than in the normal cell line (Fig. 3A). Next, the protein expression levels of MRPL14 were also examined in thyroid cancer cell lines. B-CPAP, KTC-1 and FRO cell lines showed higher MRPL14 expression than observed in the normal cell line (Fig. 3B). Because MRPL14 was a hit obtained through PTC patients in the TCGA cohort, we performed various experiments with the PTC cell lines, B-CPAP and KTC-1 for this study. To identify whether MRPL14 expression could influence the proliferation of thyroid cancer cell lines, B-CPAP and KTC-1 cells were transfected with siRNA against MRPL14 (siMRPL14-#1, #2) or an over-vector against MRPL14 (pCMV6-MRPL14). After confirming that MRPL14 siRNA specifically down-regulated MRPL14 (Fig. 3C and D), cell proliferation was detected by the CCK-8 assay. MRPL14 knockdown reduced the proliferation, whereas MRPL14 overexpression increased the proliferation of thyroid cancer cells (Fig. 3E and F, Supplementary Fig. 1A and B). Next, to determine whether MRPL14 regulated the proliferation of thyroid cancer by regulating apoptosis signaling, we investigated the expression of anti- or pro-apoptotic proteins. MRPL14 knockdown caused an increase in pro-apoptotic proteins, including cleaved caspase-3 and Bax, and a decrease in an anti-apoptotic protein (Bcl-xl), while MRPL14 overexpression showed the opposite tendency (Fig. 3G and H, Supplementary Fig. 1C). These results propose that MRPL14 could promote proliferation by regulating apoptotic proteins in thyroid cancer cells. Cell migration and invasion are crucial steps in tumor metastasis. Therefore, we investigated whether MRPL14 influences the metastatic behavior of thyroid cancer. MRPL14 knockdown significantly suppressed the migration and invasion of thyroid cancer cells compared to the control group, while MRPL14 overexpression showed the opposite tendency (Fig. 3I-L, Supplementary Fig. 1D). These results clearly display that MRPL14 promotes the migration and invasion of thyroid cancer cells. The epithelial-mesenchymal transition (EMT), which refers to a change in the cell phenotype from epithelial to mesenchymal morphology, is a vital process for the initiation and progression of tumorigenesis and metastasis [18]. To investigate whether MRPL14 could regulate EMT, we examined EMT-related proteins (Slug, Snail, E-cadherin, N-cadherin, and vimentin) by im-

Table 1. Comparison of clinicopathologic findings according to the *MRPL14* mRNA expression level in the thyroid cancer cohort

Variable	No. of patients	*MRPL14* expression		*P*-value
		Low (bottom 25%, n=125)	High (top 25%, n=125)	
Age (yr)		50.9±16.2	46.6±17.2	0.044*
Sex				0.579
Male	74	35 (28.0)	39 (31.2)	
Female	176	90 (72.0)	88 (68.8)	
Tumor size (mm)		15.5±11.4	14.2±10.3	0.329
T stage				0.000*
T1–T2	160	94 (75.2)	66 (52.8)	
T3–T4	90	31 (24.8)	59 (47.2)	
Multifocality				0.307
No	122	55 (44.0)	67 (53.6)	
Yes	123	67 (53.6)	56 (44.8)	
Unknown	5	3 (2.4)	2 (1.6)	
Extrathyroidal extension				0.000*
No	184	109 (87.2)	75 (60.0)	
Minimal	56	13 (10.4)	43 (34.4)	
Moderate/advanced	10	3 (2.4)	7 (5.6)	
Lymph node metastasis				0.000*
No	114	92 (73.6)	52 (41.6)	
N1a	72	22 (17.6)	50 (40.0)	
N1b	34	11 (8.8)	23 (18.4)	
M stage				0.561
M0	247	124 (99.2)	123 (98.4)	
M1	3	1 (0.8)	2 (1.6)	
Stage				0.000*
I	134	69 (55.2)	65 (52.0)	
II	31	25 (20.0)	6 (4.8)	
III	56	21 (16.8)	35 (28.0)	
IV	29	10 (8.0)	19 (15.2)	
Recurrence				0.605
No	234	118 (94.4)	116 (92.8)	
Yes	16	7 (5.6)	9 (7.2)	
BRAF^{V600E} mutation				0.052
No	153	84 (67.2)	69 (56.8)	
Yes	97	41 (32.8)	56 (44.8)	

Values are presented as mean±standard deviation or number (%). *P*-values from the unpaired *t*-tests for continuous parametric variables and the Mann-Whitney *U*-test for nonparametric variables. The chi-square test and Fisher exact test were used to evaluate the significance of the correlations of *MRPL14* expression with clinical and pathological parameters. The TNM classification from American Joint Committee on Cancer seventh edition was used.

*$P<0.05$ between the two categories for a given variable.

munoblot analysis. MRPL14 knockdown significantly restrained the EMT by upregulating the expression of an epithelial marker (E-cadherin) and downregulating the expression of mesenchymal markers (N-cadherin, vimentin) and transcription factors (Slug, Snail), while MRPL14 overexpression showed the opposite tendency (Fig. 3M and N, Supplementary Fig. 1E). Collectively, these results indicate that MRPL14 positively regulates thyroid cancer cell growth and metastasis.

MRPL14 knockdown inhibits the expression of OXPHOS proteins and increases intracellular ROS in thyroid cancer cell lines

In a previous study, knockdown of some MRPs caused mitochondrial OXPHOS impairment, mitochondrial dysfunction, and increased production of ROS, which are related to cancer cell death [19]. Therefore, we hypothesized that MRPL14 knockdown could decrease the activity of the OXPHOS complex and increase ROS levels in thyroid cancer. We examined the expression of OXPHOS complex proteins (ATP5A, UQCRC2, MTCO1, SDHA, NDUFA9) and ROS levels after downregulation of MRPL14 in B-CPAP and KTC-1 cell lines. MRPL14 knockdown by siRNA significantly suppressed the OXPHOS complex IV protein MTCO1 without affecting other complex proteins (Fig. 4A and B). MRPL14 knockdown also showed increased intracellular ROS in B-CPAP and KTC-1 cell lines, indicating the contribution of MRPL14 to ROS (Fig. 4C and D). These results imply that MRPL14 regulates OXPHOS complexes and the production of ROS in thyroid cancer cells. Based on the results of *in vitro* results, we investigated the relationship between MRPL14 expression and ROS-related genes using data from the CNUH cohort. GSEA analysis revealed that high MRPL14 expression was associated with enrichment of negative regulation of response to ROS and oxidative stress gene sets (Fig. 4E and F). We also confirmed that MRPL14 and the ROS inhibitory genes RACK1, PINK1 were highly positively correlated (Pearson correlation coefficient: 0.879 for *RACK1*, 0.875 for *PINK*; $P<0.01$, n=182) (Fig. 4G and H).

N-acetylcysteine restores cell proliferation and migration reduced by MRPL14 knockdown in thyroid cancer cell lines

Moderate increases of ROS are associated with various pathologic conditions, including tumor promotion and progression. However, excess ROS can cause programmed cell death. In particular, mitochondrial ROS have been reported to promote cell death [20]. As demonstrated in Fig. 4, thyroid cancer cells treated with siMRPL14 displayed higher ROS levels than the control group. Therefore, we investigated whether the reduction in proliferation and metastasis of thyroid cancer by MRPL14 downregulation was induced by ROS. N-acetylcysteine (NAC), an antioxidant drug that acts as a ROS scavenger, was used to further analyze the decrease in ROS. Co-treatment with NAC restored the ROS levels that had been increased by MRPL14 knockdown (Fig. 5A and B). As shown in Fig. 5C and D, cell proliferation inhibition induced by siMRPL14 was restored by combined treatment with NAC in B-CPAP and KTC-1 cells. NAC also restored the expression of apoptosis-related proteins altered by MRPL14 downregulation (Fig. 5E and F). Our findings collectively reveal that MRPL14 knockdown generated ROS and the generated ROS reduced cell proliferation by regulating apoptotic pathways in thyroid cancer cell lines. Given the potential inhibitory effect of ROS on the metastasis of thyroid cancer, we investigated whether NAC could also restore metastasis in thyroid cancer cells. Af-

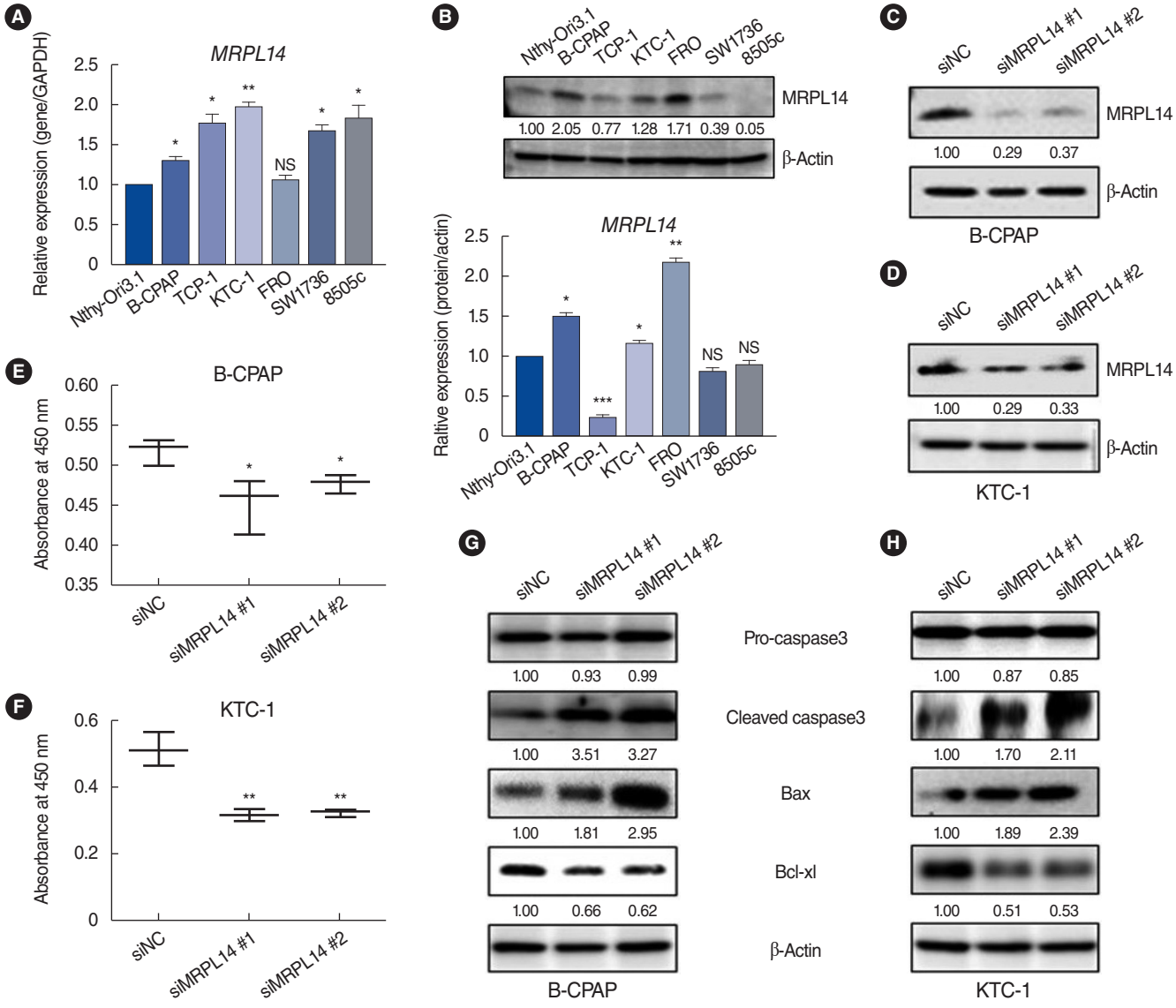

Fig. 3. *MRPL14* knockdown affects the progression of papillary thyroid cancer cells. (A) The expression of *MRPL14* mRNA in thyroid cancer cell lines was examined by real-time polymerase chain reaction. (B) The expression of mitochondrial ribosomal protein L14 (MRPL14) protein in thyroid cancer cell lines was examined by Western blot analysis. B-CPAP (C) and KTC-1 (D) cells were transfected with small interfering RNA (siRNA) targeting *MRPL14* #1, #2 or negative control siRNA for 48 hours. (E, F) After siRNA against MRPL14 (siMRPL14) transfection, cell proliferation was analyzed using the CCK-8 proliferation assay. (G, H) The expression of Caspase3, Bax and Bcl-xl were examined by Western blot analysis.

(*Continued to the next page*)

ter B-CPAP and KTC-1 cells were co-treated with siMRPL14 and NAC, the cells were permitted to migrate for 24 hours in transwell chambers. ROS inhibition by NAC significantly reversed the effect of MRPL14 suppression on migration (Fig. 5G and H). We also examined whether NAC could regulate EMT-related proteins. Co-treatment with siMRPL14 and NAC restored the effect of MRPL14 knockdown on the expression of EMT-related proteins (Fig. 5I and J). These results show that ROS accumulation induced by MRPL14 knockdown inhibited thyroid cancer metastasis through EMT signaling.

DISCUSSION

Mitochondria, often called "the powerhouses of the cell," play crucial roles in the energy metabolism of eukaryotic cells. Mitochondria also regulate important cellular processes, including metabolic adaptation, proliferation, and death in cells. Mitochondrial dysfunction and dysregulation have been reported to induce carcinogenesis and are well-known hallmarks of many cancers [21]. Some reports have investigated changes in mitochondrial proteins induced by anti-cancer drugs. An anti-colorectal cancer drug, IR-58, which exhibits significant selective killing

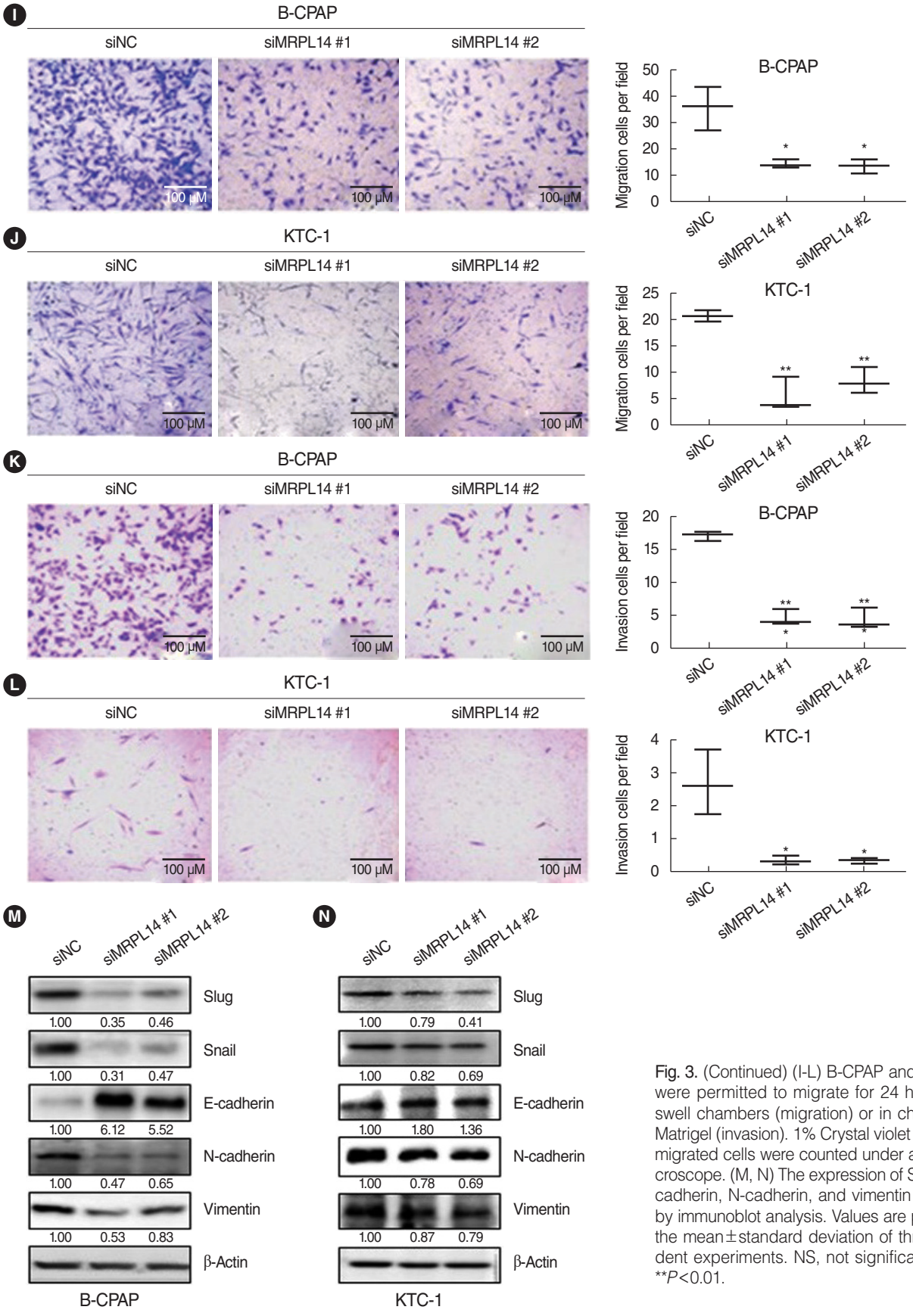

Fig. 3. (Continued) (I-L) B-CPAP and KTC-1 cells were permitted to migrate for 24 hours in transwell chambers (migration) or in chambers with Matrigel (invasion). 1% Crystal violet staining. The migrated cells were counted under an optical microscope. (M, N) The expression of Slug, Snail, E-cadherin, N-cadherin, and vimentin was studied by immunoblot analysis. Values are presented as the mean±standard deviation of three independent experiments. NS, not significant. *P<0.05, **P<0.01.

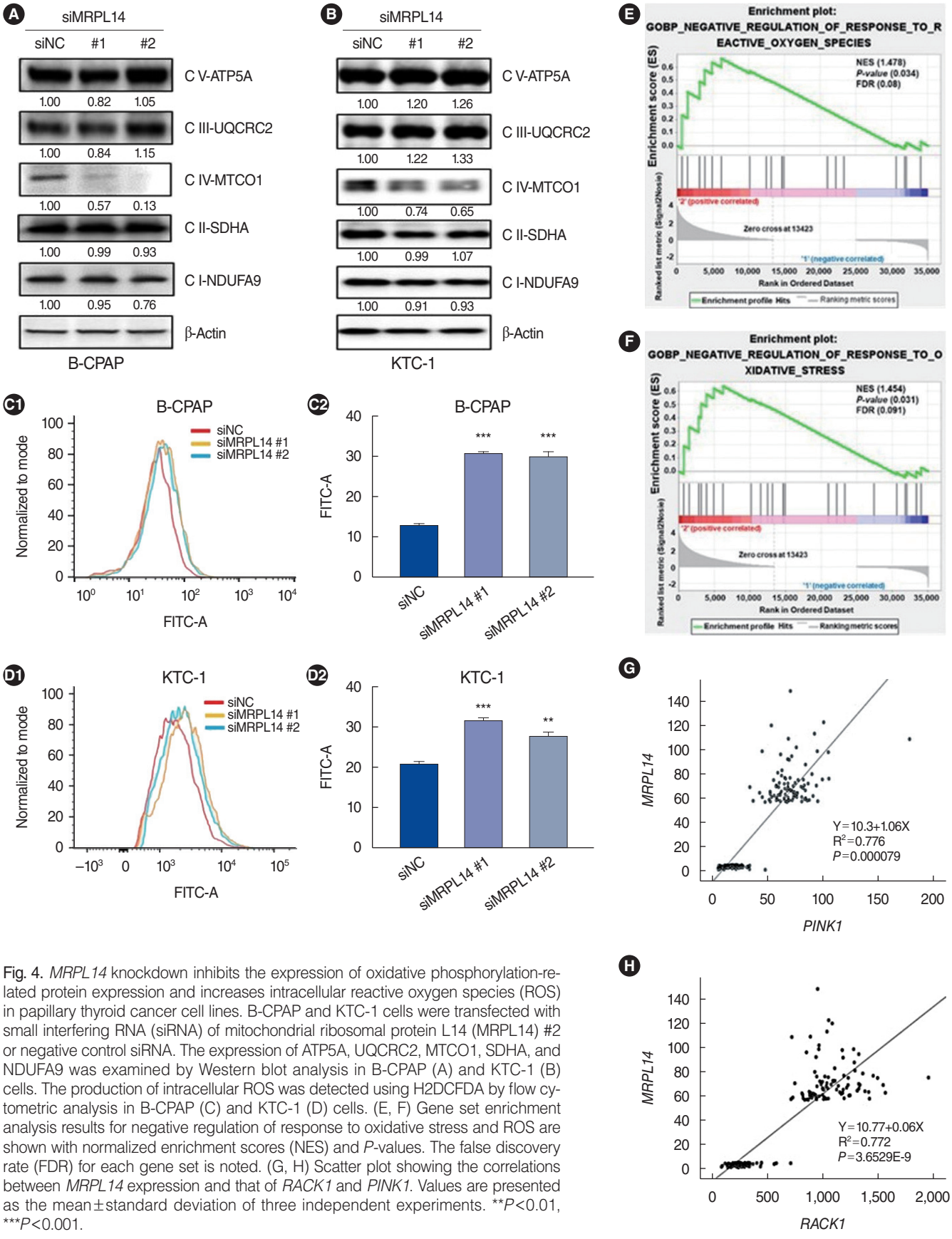

Fig. 4. *MRPL14* knockdown inhibits the expression of oxidative phosphorylation-related protein expression and increases intracellular reactive oxygen species (ROS) in papillary thyroid cancer cell lines. B-CPAP and KTC-1 cells were transfected with small interfering RNA (siRNA) of mitochondrial ribosomal protein L14 (MRPL14) #2 or negative control siRNA. The expression of ATP5A, UQCRC2, MTCO1, SDHA, and NDUFA9 was examined by Western blot analysis in B-CPAP (A) and KTC-1 (B) cells. The production of intracellular ROS was detected using H2DCFDA by flow cytometric analysis in B-CPAP (C) and KTC-1 (D) cells. (E, F) Gene set enrichment analysis results for negative regulation of response to oxidative stress and ROS are shown with normalized enrichment scores (NES) and *P*-values. The false discovery rate (FDR) for each gene set is noted. (G, H) Scatter plot showing the correlations between *MRPL14* expression and that of *RACK1* and *PINK1*. Values are presented as the mean±standard deviation of three independent experiments. ***P*<0.01, ****P*<0.001.

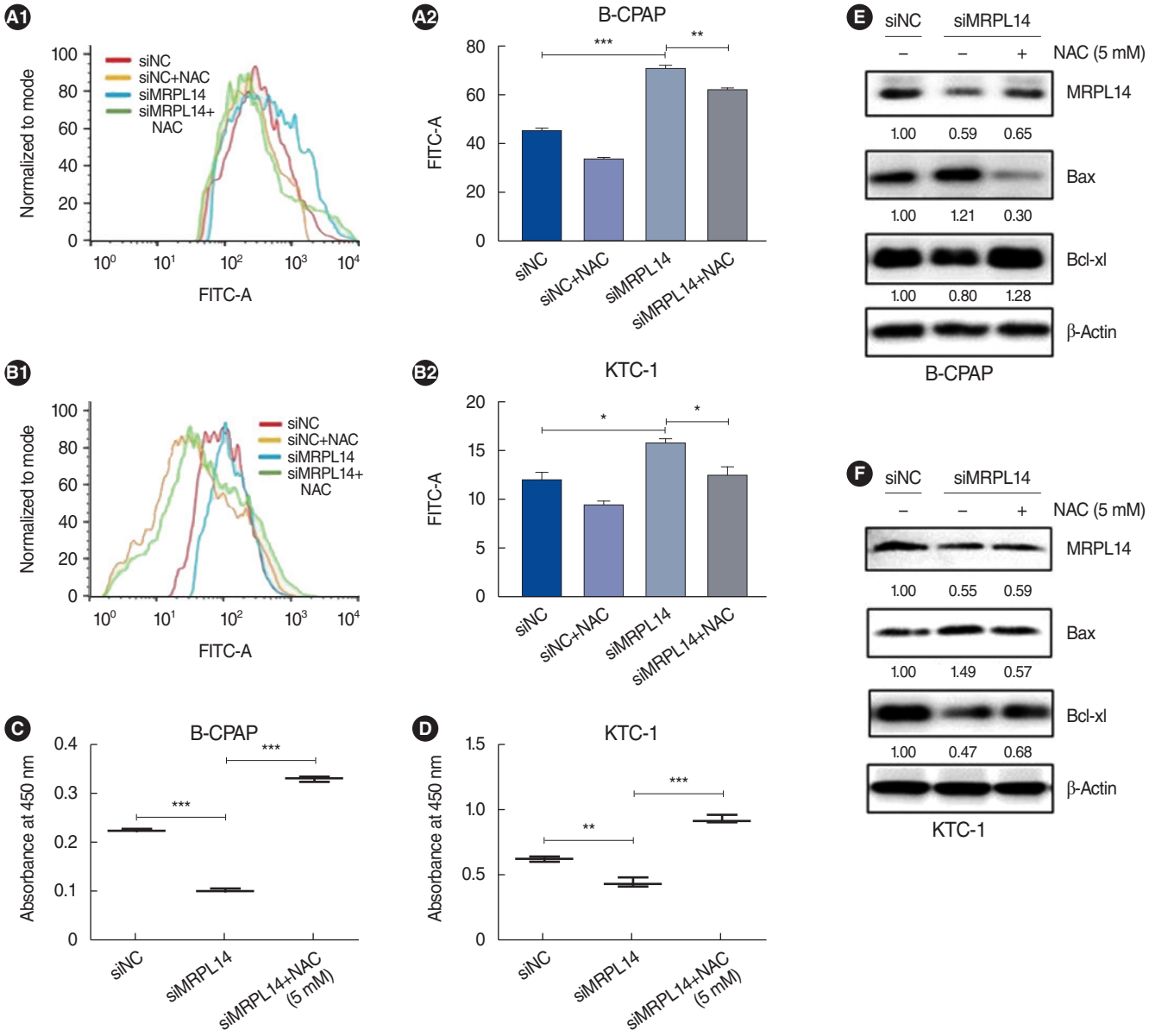

Fig. 5. N-acetylcysteine (NAC) restores cell progression reduced by *MRPL14* knockdown in papillary thyroid cancer cell lines. B-CPAP and KTC-1 cells were transfected with small interfering RNA (siRNA) of mitochondrial ribosomal protein L14 (MRPL14) #2 or negative control siRNA and co-treated with NAC for 48 hours. (A, B) Flow cytometric histogram shows intracellular reactive oxygen species in siMRPL14 transfection and NAC treated cell lines. (C, D) Cell proliferation was analyzed using a CCK-8 proliferation assay. (E, F) The expression of Bax and Bcl-xl were examined by immunoblot analysis.
(*Continued to the next page*)

effects against tumors, downregulates the expression of mitochondrial protein translocase TIM44 [22]. It has also been reported that itraconazole, a clinically used antifungal drug, possesses potent antiangiogenic and anticancer activity, and it can inhibit mitochondrial protein VDAC1 to disrupt mitochondrial metabolism [23]. Given these vital roles of mitochondria in cancer cells, more mitochondria-focused cancer research is needed.

MRPs are important for mitochondrial-encoded protein synthesis and mitochondrial function. MRPs also involved in the process of cell proliferation, apoptosis, and metastasis [24]. Recent studies have revealed that abnormal expression of MRPs and their encoding genes is related to cancer development and progression [10]. MRPL41 overexpression contributes to p53 stability and induces apoptosis in various cancer [25]. MRPS36 induces cell cycle arrest and cell proliferation inhibition through p53 modification and p21 expression [26]. MRPS16 facilitates growth, migration, and invasion in glioma cells by activating the PI3K/AKT/Snail signaling axis [13]. As such, although studies on the mechanism of some MRPs in cancer have been conducted, much remains unknown regarding the expression states and

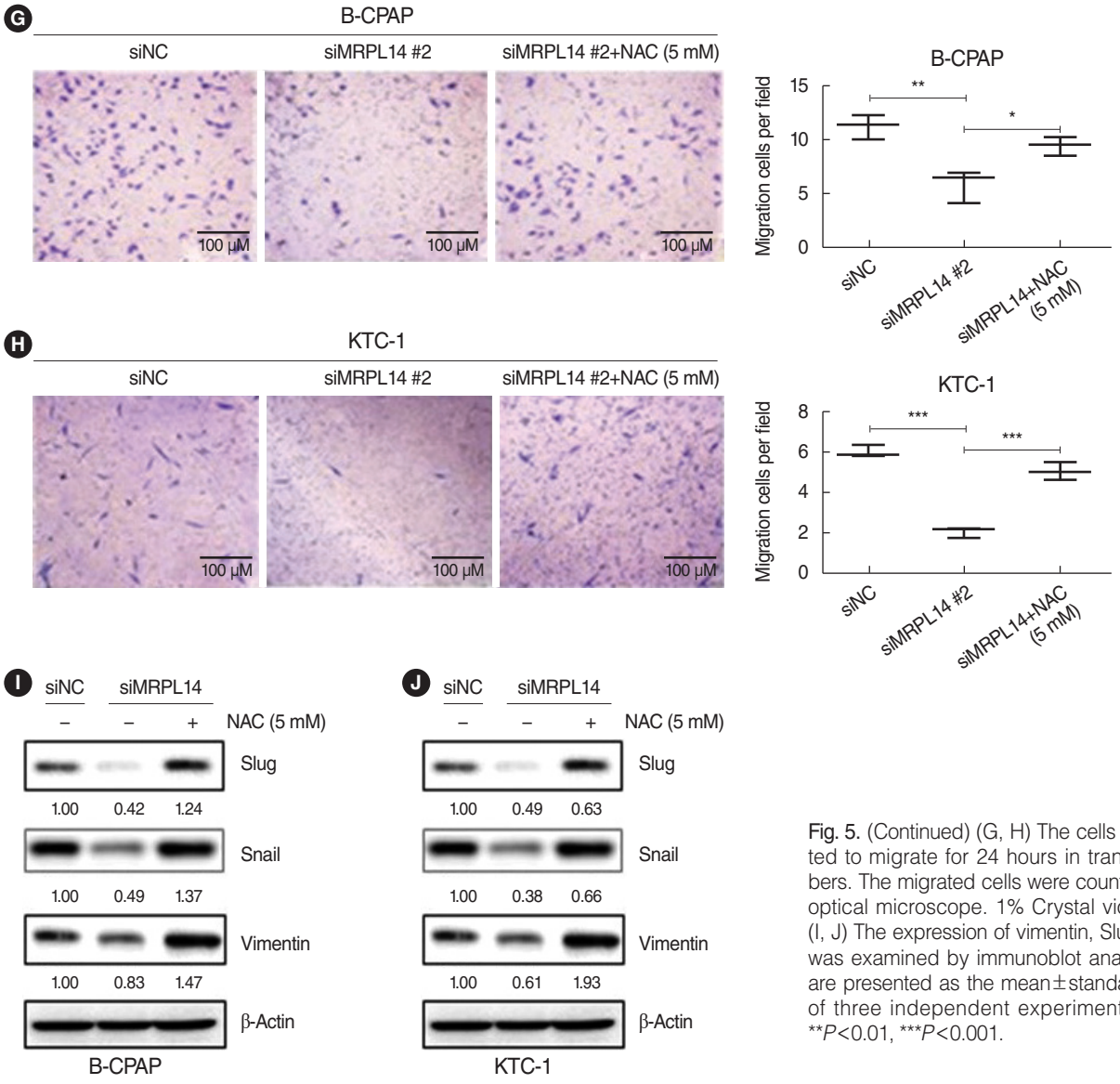

Fig. 5. (Continued) (G, H) The cells were permitted to migrate for 24 hours in transwell chambers. The migrated cells were counted under an optical microscope. 1% Crystal violet staining. (I, J) The expression of vimentin, Slug, and Snail was examined by immunoblot analysis. Values are presented as the mean±standard deviation of three independent experiments. **P*<0.05, ***P*<0.01, ****P*<0.001.

specific regulatory mechanism of MRPL14 in cancer, peculiarly in thyroid cancer.

First, to investigate the MRPs that affect thyroid cancer progression, we analyzed the expression pattern of MRPs in thyroid cancer (PTC) using the TCGA database. Among up-MRPs with potential as oncogenes, MRPL14 was the most upregulated gene, with dramatically increased expression in thyroid cancer compared to normal. The TCGA data showed that high MRPL14 expression was associated with a more aggressive phenotype, including advanced T stage, lymph node metastasis, and extrathyroidal extension. Although high expression of MRPL14 was also correlated with unfavorable disease-free survival and overall survival in thyroid cancer, those relationships were not statistically significant (data not shown). In addition to the TCGA cohort, we performed transcriptomic analysis using the CNUH cohort. MRPL14 expression was also upregulated in PTC tumor samples compared to normal samples. Data from both the TCGA database and the CNUH cohort indicated that high expression of MRPL14 was strongly associated with tumor aggressiveness in thyroid cancer.

In this study, we observed the function of MRPL14 in thyroid cancer in an *in vitro* studies using PTC cell lines. We discovered that MRPL14 was highly expressed in various thyroid cancer cell lines and *MRPL14* knockdown obviously suppressed cell growth, migration, and invasion in PTC cell lines. To explore the mechanism of MRPL14 in promoting thyroid cancer progression and metastasis, we focused on the intrinsic role of MRPL14, which is a key component of the mitochondrial translation machinery. MRPs are functionally responsible for the translation of OXPHOS complex-related proteins, which supply energy for cell survival and metabolism [27]. Recent studies have demonstrated that downregulation of MRPs caused OXPHOS impair-

ment and induced the generation of ROS [19]. In our study, *MRPL14* knockdown reduced the expression of the OXPHOS complex IV protein MTCO1, encoded in the mitochondrial DNA, and increased ROS production, leading to cell death. This result indicates that MRPL14-mediated OXPHOS regulation may induce PTC cell death via ROS production.

At normal levels, ROS plays a pivotal role in cellular processes, whereas excess levels of ROS cause oxidative damage to proteins and DNA and result in cell death (i.e., apoptosis) [28]. A small increase of ROS is related to the initiation and progression of cancer, but a substantial increase in ROS can induce apoptosis and suppress tumor progression and metastasis [20]. Here, we showed that MRPL14 knockdown induced ROS accumulation and suppressed the proliferation by regulating the apoptotic proteins of thyroid cancer cells. MRPL14 knockdown also inhibited cell migration and invasion by blocking the EMT in thyroid cancer cells. Furthermore, NAC, a general antioxidant, reversed the effect of MRPL14 knockdown on cell proliferation and migration. These findings indicate that MRPL14 promotes cell growth, migration, and invasion through modulating ROS in thyroid cancer.

Recent studies have revealed that several cytosolic ribosomal proteins regulate therapeutic resistance in various cancers [29]. For instance, the knockdown of ribosomal protein S27a (RPS27A) improved the therapeutic efficacy of the tyrosine kinase inhibitor imatinib in chronic myeloid leukemia [30]. Silencing of ribosomal protein large P (RPLP) promoted apoptosis and decreased radio-resistance *in vitro* in HNSCC [31]. Furthermore, MRPL33 enhanced the sensitivity of gastric cancer cells to epirubicin, a chemotherapy drug [32]. This evidence implies that the combined treatment with chemotherapy or radiotherapy and MRPL14 knockdown could enhance the anticancer effect. Further research on this combined treatment effect is needed in the future.

In our study, the function of MRPL14 on thyroid cancer and its mechanisms were limited to PTC. We studied the importance of MRPL14 in B-CPAP and KTC-1 cells harboring the $BRAF^{V600E}$ mutation, which correlates with a more aggressive type of thyroid cancer. Furthermore, MRPL14 may also be associated with poorly-differentiated ATC or even RAI-refractory PTC. We plan to investigate this in further studies. Furthermore, in order to advance the treatment of thyroid cancer, it is necessary to investigate which signaling pathways are involved in the role of MRPL14 in thyroid cancer.

In conclusion, we discovered the oncogenicity of MRPL14 in the development of thyroid cancer. MRPL14 was highly expressed in PTC and promoted thyroid cancer progression and metastasis through the regulation of OXPHOS complex IV protein MTCO1 and ROS modulation. Our findings indicate that MRPL14 might serve as an independent prognostic factor for thyroid cancer. To our knowledge, this is the first report demonstrating the mechanism of action of MRPL14 as an oncogene in thyroid cancer.

CONFLICT OF INTEREST

Bon Seok Koo is an editorial board member of the journal but was not involved in the peer reviewer selection, evaluation, or decision process of this article. No other potential conflicts of interest relevant to this article were reported.

ACKNOWLEDGMENTS

We thank Professor Yea Eun Kang (Chungnam University) for kindly providing Nthy-ori3.1. This study was supported by the research fund of Chungnam National University and the BK21 FOUR Program by Chungnam National University Research Grant, 2021, and a grant of the Korea Health Technology R&D Project through the Korea Health Industry Development Institute (KHIDI), funded by the Ministry of Health & Welfare, Republic of Korea (grant no. HR20C0025, HR22C1734) and the National Research Foundation of Korea (NRF) (grant no. 2019R1A2C1084125, 2018R1D1A1B07050825). This work was supported by a Korea Medical Device Development Fund grant funded by the Korean government (the Ministry of Science and ICT, the Ministry of Trade, Industry and Energy, the Ministry of Health & Welfare, the Ministry of Food and Drug Safety) (project no. 1711138229, KMDF_PR_20200901_0124). This work was also supported by BK21 FOUR Program by Chungnam National University Research Grant, 2022.

ORCID

Hae Jong Kim https://orcid.org/0000-0002-2735-4154
Quoc Khanh Nguyen https://orcid.org/0000-0002-0046-0475
Seung-Nam Jung https://orcid.org/0000-0002-2636-8343
Mi Ae Lim https://orcid.org/0000-0003-2395-4272
Chan Oh https://orcid.org/0000-0002-5366-8333
Yudan Piao https://orcid.org/0000-0002-5622-5925
YanLi Jin https://orcid.org/0000-0003-3102-5748
Ju-Hui Kim https://orcid.org/0000-0001-7645-5683
Young Il Kim https://orcid.org/0000-0003-3696-7187
Yea Eun Kang https://orcid.org/0000-0002-2012-3716
Jae Won Chang https://orcid.org/0000-0002-6596-931X
Ho-Ryun Won https://orcid.org/0000-0002-5135-2474
Bon Seok Koo https://orcid.org/0000-0002-5928-0006

AUTHOR CONTRIBUTIONS

Conceptualization: BSK, HJK, QKN. Methodology: HJK, MAL, CO, YP. Software: QKN. Validation: QKN. Formal analysis: QKN. Investigation: HJK, YLJ. Data curation: HJK, QKN, MAL, JHK. Visualization: CO, YP, YLJ. Supervision: YIK, YEK, JWC, HRW.

Project administration: YIK, YEK, JWC, HRW, BSK. Funding acquisition: BSK. Writing–original draft: HJK, SNJ. Writing–review & editing: SNJ, BSK.

SUPPLEMENTARY MATERIALS

Supplementary materials can be found online at https://doi.org/10.21053/ceo.2022.01760.

REFERENCES

1. Ancker OV, Kruger M, Wehland M, Infanger M, Grimm D. Multikinase inhibitor treatment in thyroid cancer. Int J Mol Sci. 2019 Dec;21(1):10.
2. Ahn SH. Usage and diagnostic yield of fine-needle aspiration cytology and core needle biopsy in thyroid nodules: a systematic review and meta-analysis of literature published by Korean authors. Clin Exp Otorhinolaryngol. 2021 Feb;14(1):116-30.
3. Park SJ, Kang YE, Kim JH, Park JL, Kim SK, Baek SW, et al. Transcriptomic analysis of papillary thyroid cancer: a focus on immune-subtyping, oncogenic fusion, and recurrence. Clin Exp Otorhinolaryngol. 2022 May;15(2):183-93.
4. Yi JW, Ha SY, Jee HG, Kim K, Kim SJ, Chai YJ, et al. Induction of the BRAFV600E mutation in thyroid cells leads to frequent hypermethylation. Clin Exp Otorhinolaryngol. 2022 Aug;15(3):273-82.
5. Zheng CM, Ji YB, Song CM, Ge MH, Tae K. Number of metastatic lymph nodes and ratio of metastatic lymph nodes to total number of retrieved lymph nodes are risk factors for recurrence in patients with clinically node negative papillary thyroid carcinoma. Clin Exp Otorhinolaryngol. 2018 Mar;11(1):58-64.
6. Neff RL, Farrar WB, Kloos RT, Burman KD. Anaplastic thyroid cancer. Endocrinol Metab Clin North Am. 2008 Jun;37(2):525-38.
7. Tang P, Dang H, Huang J, Xu T, Yuan P, Hu J, et al. NADPH oxidase NOX4 is a glycolytic regulator through mROS-HIF1α axis in thyroid carcinomas. Sci Rep. 2018 Oct;8(1):15897.
8. Kim HJ, Maiti P, Barrientos A. Mitochondrial ribosomes in cancer. Semin Cancer Biol. 2017 Dec;47:67-81.
9. Yan C, Duanmu X, Zeng L, Liu B, Song Z. Mitochondrial DNA: distribution, mutations, and elimination. Cells. 2019 Apr;8(4):379.
10. Huang G, Li H, Zhang H. Abnormal expression of mitochondrial ribosomal proteins and their encoding genes with cell apoptosis and diseases. Int J Mol Sci. 2020 Nov;21(22):8879.
11. Sorensen KM, Meldgaard T, Melchjorsen CJ, Fridriksdottir AJ, Pedersen H, Petersen OW, et al. Upregulation of Mrps18a in breast cancer identified by selecting phage antibody libraries on breast tissue sections. BMC Cancer. 2017 Jan;17(1):19.
12. Koc EC, Haciosmanoglu E, Claudio PP, Wolf A, Califano L, Friscia M, et al. Impaired mitochondrial protein synthesis in head and neck squamous cell carcinoma. Mitochondrion. 2015 Sep;24:113-21.
13. Wang Z, Li J, Long X, Jiao L, Zhou M, Wu K. MRPS16 facilitates tumor progression via the PI3K/AKT/Snail signaling axis. J Cancer. 2020 Feb;11(8):2032-43.
14. Oviya RP, Gopal G, Shirley SS, Sridevi V, Jayavelu S, Rajkumar T. Mitochondrial ribosomal small subunit proteins (MRPS) MRPS6 and MRPS23 show dysregulation in breast cancer affecting tumorigenic cellular processes. Gene. 2021 Jul;790:145697.
15. Fung S, Nishimura T, Sasarman F, Shoubridge EA. The conserved interaction of C7orf30 with MRPL14 promotes biogenesis of the mitochondrial large ribosomal subunit and mitochondrial translation. Mol Biol Cell. 2013 Feb;24(3):184-93.
16. Trapnell C, Roberts A, Goff L, Pertea G, Kim D, Kelley DR, et al. Differential gene and transcript expression analysis of RNA-seq experiments with TopHat and Cufflinks. Nat Protoc. 2012 Mar;7(3):562-78.
17. Ferreira JA, Zwinderman AH. On the benjamini-hochberg method. Ann Statist. 2006 Aug;34:1827-49.
18. van Zijl F, Krupitza G, Mikulits W. Initial steps of metastasis: cell invasion and endothelial transmigration. Mutat Res. 2011 Jul-Oct;728(1-2):23-34.
19. Zhang L, Lu P, Yan L, Yang L, Wang Y, Chen J, et al. MRPL35 is upregulated in colorectal cancer and regulates colorectal cancer cell growth and apoptosis. Am J Pathol. 2019 May;189(5):1105-20.
20. Perillo B, Di Donato M, Pezone A, Di Zazzo E, Giovannelli P, Galasso G, et al. ROS in cancer therapy: the bright side of the moon. Exp Mol Med. 2020 Feb;52(2):192-203.
21. Liu Y, Shi Y. Mitochondria as a target in cancer treatment. MedComm (2020). 2020 Jul;1(2):129-39.
22. Huang Y, Zhou J, Luo S, Wang Y, He J, Luo P, et al. Identification of a fluorescent small-molecule enhancer for therapeutic autophagy in colorectal cancer by targeting mitochondrial protein translocase TIM44. Gut. 2018 Feb;67(2):307-19.
23. Head SA, Shi W, Zhao L, Gorshkov K, Pasunooti K, Chen Y, et al. Antifungal drug itraconazole targets VDAC1 to modulate the AMPK/mTOR signaling axis in endothelial cells. Proc Natl Acad Sci U S A. 2015 Dec;112(52):E7276-85.
24. Richter U, Lahtinen T, Marttinen P, Myohanen M, Greco D, Cannino G, et al. A mitochondrial ribosomal and RNA decay pathway blocks cell proliferation. Curr Biol. 2013 Mar;23(6):535-41.
25. Yoo YA, Kim MJ, Park JK, Chung YM, Lee JH, Chi SG, et al. Mitochondrial ribosomal protein L41 suppresses cell growth in association with p53 and p27Kip1. Mol Cell Biol. 2005 Aug;25(15):6603-16.
26. Chen YC, Chang MY, Shiau AL, Yo YT, Wu CL. Mitochondrial ribosomal protein S36 delays cell cycle progression in association with p53 modification and p21(WAF1/CIP1) expression. J Cell Biochem. 2007 Mar;100(4):981-90.
27. Sotgia F, Whitaker-Menezes D, Martinez-Outschoorn UE, Salem AF, Tsirigos A, Lamb R, et al. Mitochondria "fuel" breast cancer metabolism: fifteen markers of mitochondrial biogenesis label epithelial cancer cells, but are excluded from adjacent stromal cells. Cell Cycle. 2012 Dec;11(23):4390-401.
28. Lin S, Li Y, Zamyatnin AA Jr, Werner J, Bazhin AV. Reactive oxygen species and colorectal cancer. J Cell Physiol. 2018 Jul;233(7):5119-32.
29. Elhamamsy AR, Metge BJ, Alsheikh HA, Shevde LA, Samant RS. Ribosome biogenesis: a central player in cancer metastasis and therapeutic resistance. Cancer Res. 2022 Jul;82(13):2344-53.
30. Wang H, Xie B, Kong Y, Tao Y, Yang G, Gao M, et al. Overexpression of RPS27a contributes to enhanced chemoresistance of CML cells to imatinib by the transactivated STAT3. Oncotarget. 2016 Apr;7(14):18638-50.
31. Chen TW, Chang KP, Cheng CC, Chen CY, Hong SW, Sie ZL, et al. Characterization of recurrent relevant genes reveals a novel role of RPL36A in radioresistant oral squamous cell carcinoma. Cancers (Basel). 2021 Nov;13(22):5623.
32. Li J, Feng D, Gao C, Zhang Y, Xu J, Wu M, et al. Isoforms S and L of MRPL33 from alternative splicing have isoform-specific roles in the chemoresponse to epirubicin in gastric cancer cells via the PI3K/AKT signaling pathway. Int J Oncol. 2019 May;54(5):1591-600.